SUPPLEMENTAL INFORMATION

Elevated CDKN1A (P21) mediates β-thalassemia erythroid apoptosis but its loss does not improve β-thalassemic erythropoiesis

Authors: Raymond Liang[1,2@*], Miao Lin[1%*], Vijay Menon[1§], Jiajing Qiu[1], Anagha Menon[1,2], Laura Breda[3], Tasleem Arif[1], Stefano Rivella[3], and Saghi Ghaffari[1,2,4,5,6#]

Affiliations: [1]Department of Cell, Developmental & Regenerative Biology, [2]Developmental and Stem Cell Biology Multidisciplinary Training, Graduate School of Biomedical Sciences, Icahn School of Medicine at Mount Sinai, New York, New York 10029, [3] Children's Hospital of Philadelphia, University of Pennsylvania, Philadelphia, PA 19104, [4]Department of Oncological Sciences, [5]Black Family Stem Cell Institute, [6]Tisch Cancer Institute, Icahn School of Medicine at Mount Sinai, New York, New York 10029

 # Correspondence: Saghi Ghaffari, M.D.-Ph.D., Department of Cell, Developmental & Regenerative Biology, Icahn School of Medicine at Mount Sinai, New York, NY 10029, Tel: 212-659-8271, Fax: 212-803-6740; e-mail: Saghi.Ghaffari@mssm.edu

Running Title: P21 regulates β-thalassemia erythroid apoptosis

@ Current position: Mnemo Therapeutics, New York, NY
% Current position: University of Rochester, Rochester, NY
§ Current position: Department of Therapeutic Radiology, Yale University, New Haven, CT
*These authors contributed equally to the work

Supplemental Figure Legends

Figure S1: Elevated ROS levels in β-thalassemic erythroid cells. (**A, B**) CM-H2DCFDA staining of TER119^{+} cells (**A**) and c-Kit^{+} CD71^{Hi} TER119$^{-/Lo/Hi}$ (**B**). Results are shown as Mean ± SEM; *p < 0.05.

Figure S2: Apoptosis in β-thalassemic erythroid cells. (**A**) FACS analysis of apoptosis in erythroid cell precursors per gate. (**B**) Overlays of Annexin V positivity in wild type versus β-thalassemic live erythroid (TER 119+) cells per Gate. (**C**) Quantification of (**B**); results normalized to wild type in each gate. Results are shown as Mean ± SEM; *p < 0.05, **p < 0.01.

Figure S3: Upregulation of FOXO3 in β-thalassemic erythroid progenitor cells. (**A**) Gating strategy of erythroid progenitors/precursors in c-Kit^{+} β-thalassemic vs. WT bone marrow cells. (**B**) qRT-PCR expression analysis of Foxo3 in gates I-IV. (**C**) FOXO3 nuclear localization in *WT* and *Hbb$^{th3/+}$* erythroid progenitors using confocal microscopy; representative images (bottom); quantification of data analyses of at least 40 cells (top). Results are shown as Mean ± SEM; *p < 0.05, **p < 0.01.

Figure S4: **Analyses of TP53 expression in β-thalassemic erythroid progenitor cells.** Representative confocal images of TP53 nuclear localization in *WT* and *Hbb$^{th3/+}$* erythroid progenitors (Top). Quantification of data (bottom). Representative data is shown as Mean ± SEM. of at least 30 cells; n.s., not significant.

Figure S5: FOXO3 mediates apoptosis in β-thalassemic erythroid precursor cells. (**A**) Frequency of Annexin V^{+} cells in live Gate IV TER119^{+} bone marrow cells from *WT*, *Foxo3$^{-/-}$*, *Hbb$^{th3/+}$* and *Foxo3$^{-/-}$/Hbb$^{th3/+}$* mice. Results are shown as Mean ± SD *p < 0.05 (between WT and *Hbb$^{th3/+}$*, $^{\#}$p < 0.05 between *Hbb$^{th3/+}$* and *Foxo3$^{-/-}$/Hbb$^{th3/+}$*). (**B**) qRT-PCR expression analysis of *Foxo1* in gates I-IV. Mean ± SEM; **p < 0.01.

Figure S6: **Loss of FOXO3 leads to ROS elevation in β-thalassemic erythroid cells.** ROS levels in BM (**A**) and spleen (**B**) erythroblast populations. Mean ± SEM; *p < 0.05, **p < 0.01 ($n \geq 3$).

Figure S7: Expression of FOXO3 target PUMA is elevated in β-thalassemic erythroid cells. (**A**) Heatmap analysis of RNA-Seq data of apoptosis-related gene cluster in Gates I-III of *WT* and *Foxo3$^{-/-}$* erythroblasts. Heatmap generated using Morpheus software (https://software.broadinstitute.org/morpheus). (**B**) qRT-PCR expression analysis of pro-apoptotic genes *Puma* and *Bim* in *Hbb$^{th3/+}$* and double mutant erythroblasts. Data is shown as Mean ± S.E.M; *p < 0.05 between *WT* and *Hbb$^{th3/+}$*; $^{\#}$p < 0.05 and $^{\#\#}$p < 0.01 between *Hbb$^{th3/+}$* and *Foxo3$^{-/-}$/Hbb$^{th3/+}$*; $^{\$}$p < 0.05 between *WT* and *Foxo3$^{-/-}$/Hbb$^{th3/+}$*. (**C**) Western blot analysis of PUMA protein expression in β-thalassemic erythroblasts (top) and quantification (bottom). Mean ± SEM; *p < 0.05 (n=3).

Figure S8: **Loss of P21 does not improve β-thalassemic erythropoiesis.** (**A**) Macroscopic examination of spleen from *WT*, *p21*$^{-/-}$, *Hbb*$^{th3/+}$, *p21*$^{-/-}$/*Hbb*$^{th3/+}$. (**B**) Spleen weight of *WT*, *p21*$^{-/-}$, *Hbb*$^{th3/+}$, and *p21*$^{-/-}$/*Hbb*$^{th3/+}$ mice from 3 mice per group. (**C**) Flow cytometric analysis of TER119 in splenocytes; n = 3 for each group. (**D**) Splenocyte count from *WT*, *p21*$^{-/-}$, *Hbb*$^{th3/+}$ and *p21*$^{-/-}$/*Hbb*$^{th3/+}$ mice from 3 mice per group. (**E**) Total number of bone marrow cells analyzed by flow cytometry, n = 3 for each group. (**F**) Total live cells within the bone marrow quantified in (**E**), n = 3 for each group. (**G**) Flow cytometric analysis of TER119 in the bone marrow, n = 3 for each group. (**H**) ROS levels in spleen erythroblasts (n = 3 mice /group). (**I**) Plasma Epo levels (n = 3 mice/group). Mean ± SD; *p < 0.05, **p < 0.01, ***p < 0.001, ****p < 0.0001.

Figure S9: Loss of P21 does not improve β-thalassemic erythroid cell maturation. Histograms showing the percentage of erythroblasts in *WT*, *p21*$^{-/-}$, *Hbb*$^{th3/+}$, *p21*$^{-/-}$/*Hbb*$^{th3/+}$ bone marrow (**A**)**,** and spleen (**B**). Mean ± SD; *p < 0.05, **p < 0.01, ***p < 0.001, ****p < 0.0001

Fig. S1

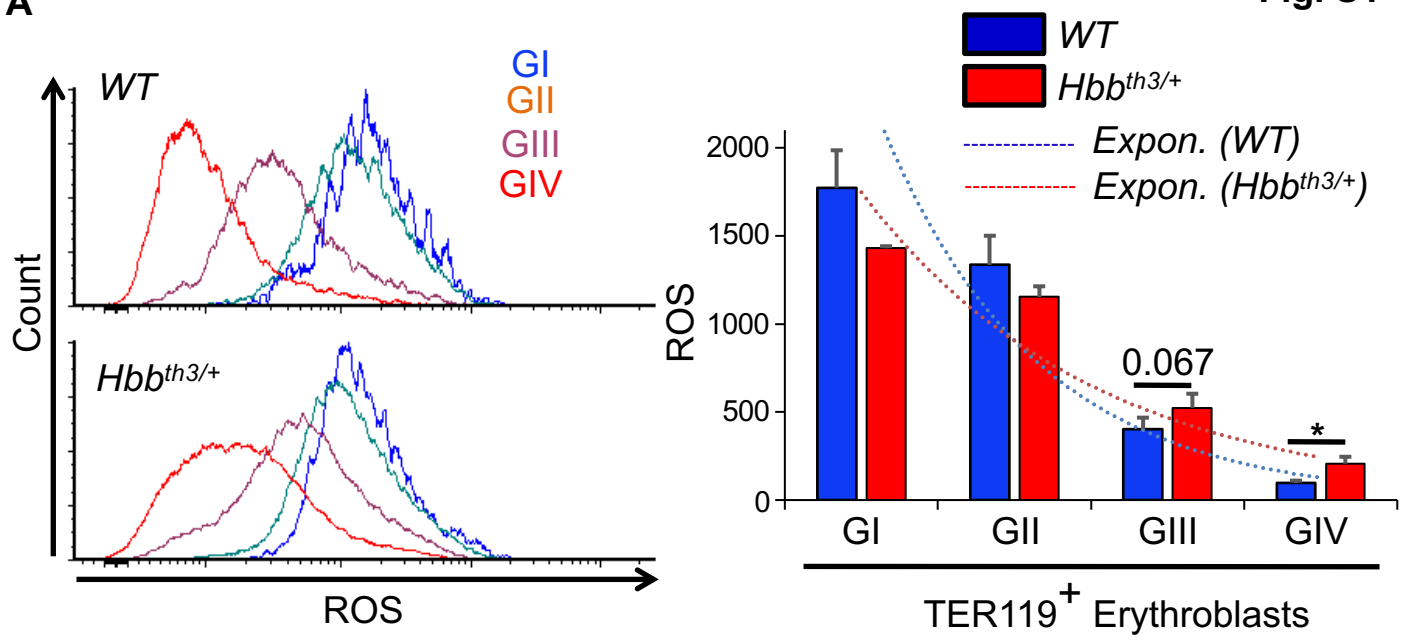
A
WT
GI
GII
GIII
GIV
Count
Hbb^th3/+
ROS
WT
Hbb^th3/+
Expon. (WT)
Expon. (Hbb^th3/+)
2000
1500
1000
500
0
ROS
0.067
*
GI
GII
GIII
GIV
TER119+ Erythroblasts

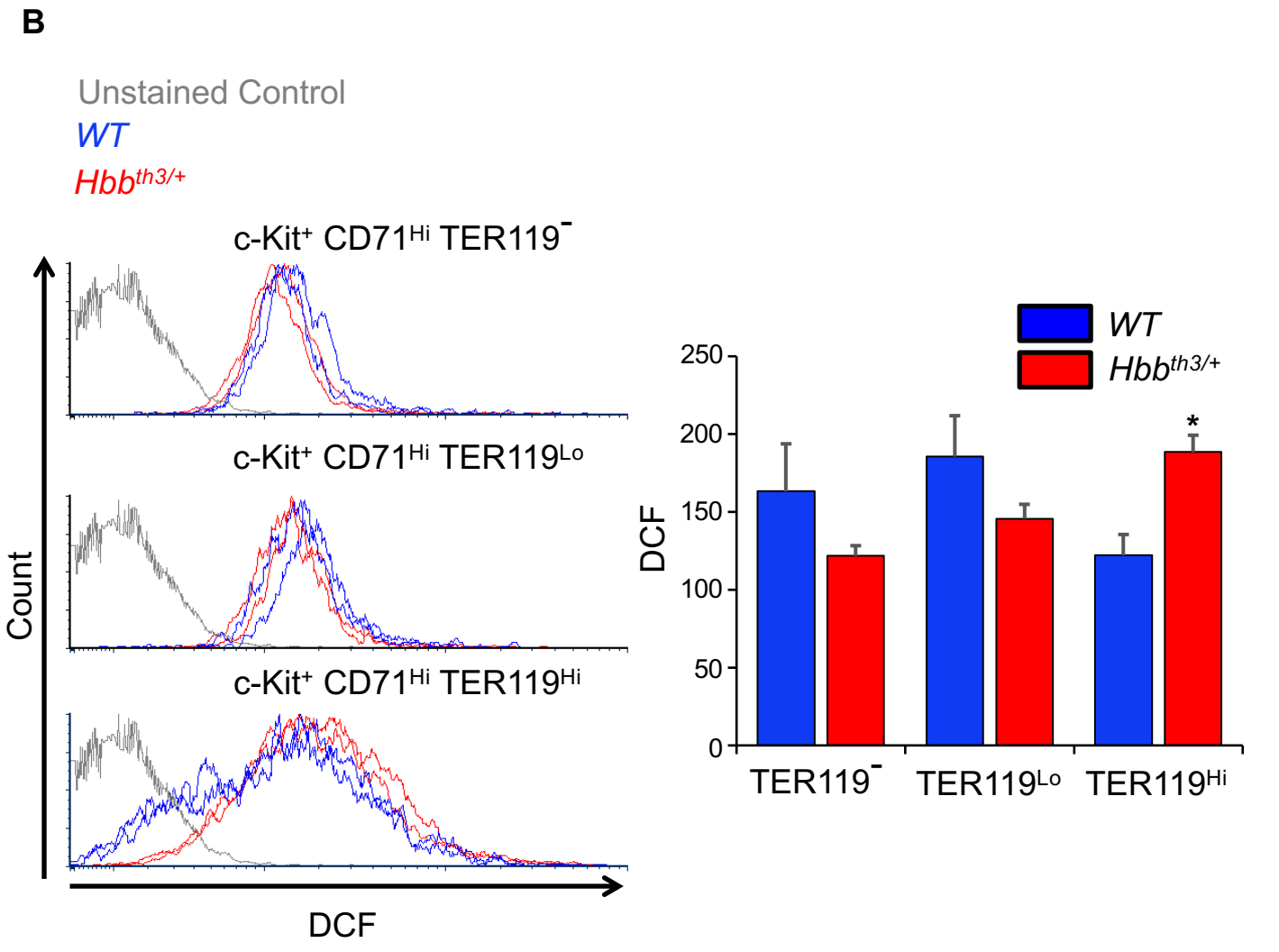
B
Unstained Control
WT
Hbb^th3/+
c-Kit+ CD71Hi TER119-
c-Kit+ CD71Hi TER119Lo
c-Kit+ CD71Hi TER119Hi
Count
DCF
WT
Hbb^th3/+
250
200
150
100
50
0
DCF
*
TER119-
TER119Lo
TER119Hi

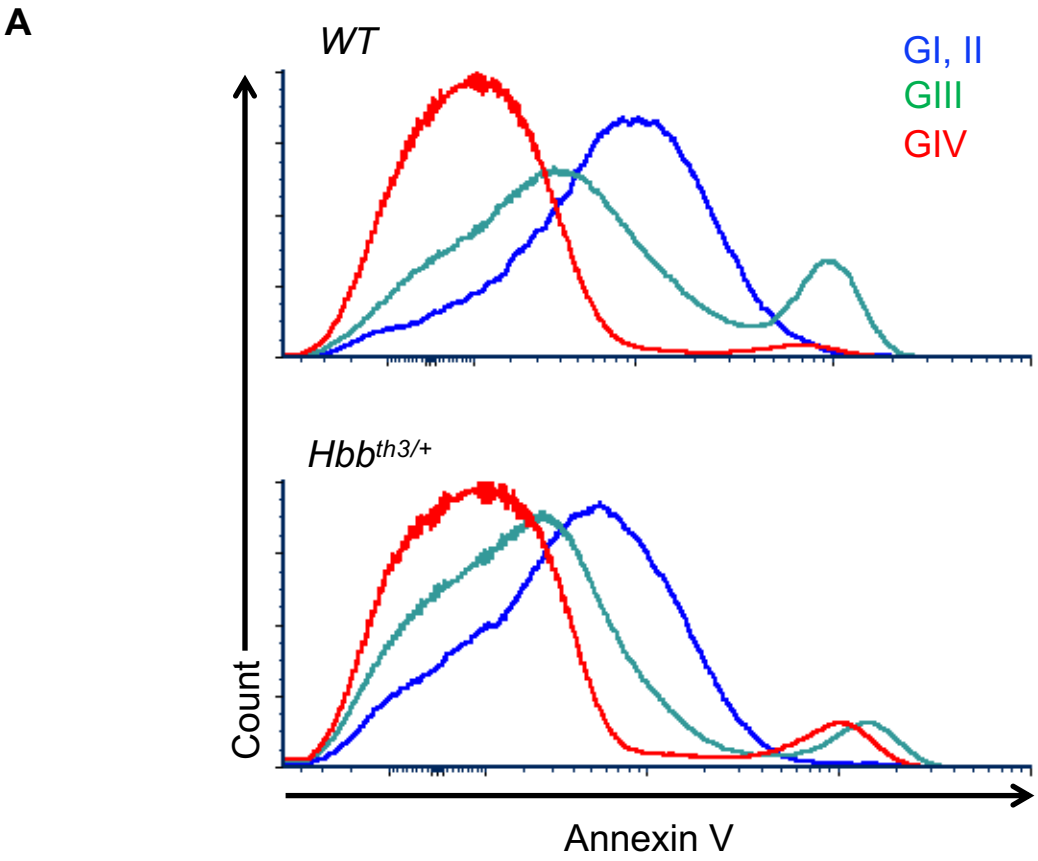
A
WT
GI, II
GIII
GIV
Hbb^th3/+
Count
Annexin V

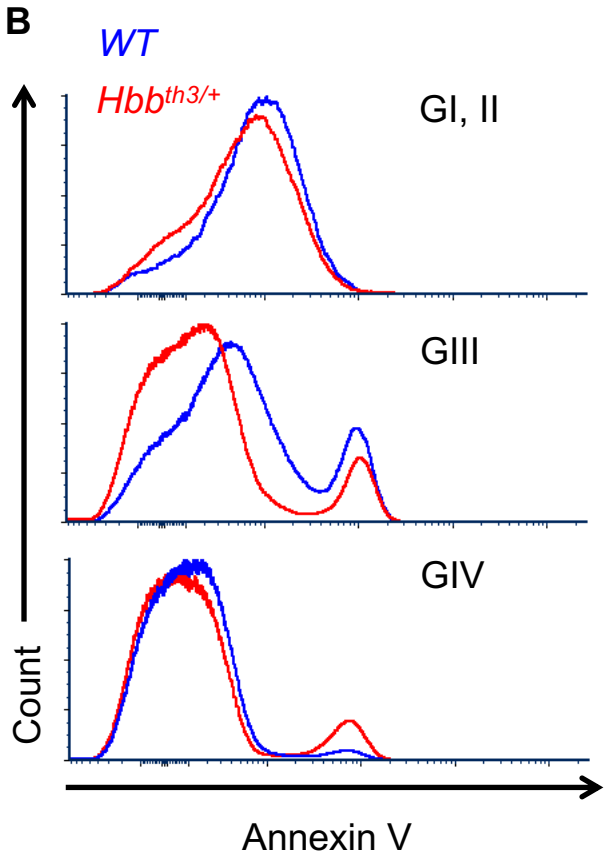
B
WT
Hbb^th3/+
GI, II
GIII
GIV
Count
Annexin V

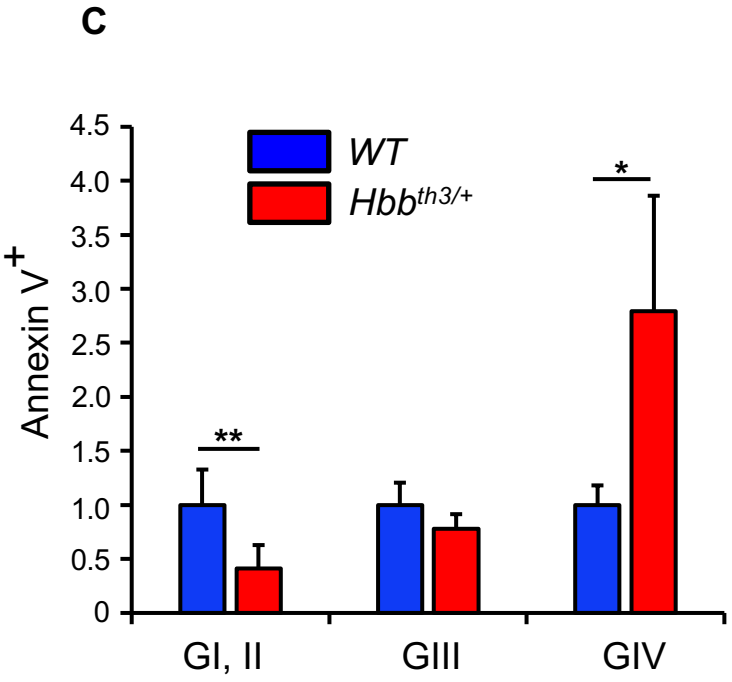
C
WT
Hbb^th3/+
Annexin V+
4.5
4.0
3.5
3.0
2.5
2.0
1.5
1.0
0.5
0
**
*
GI, II
GIII
GIV

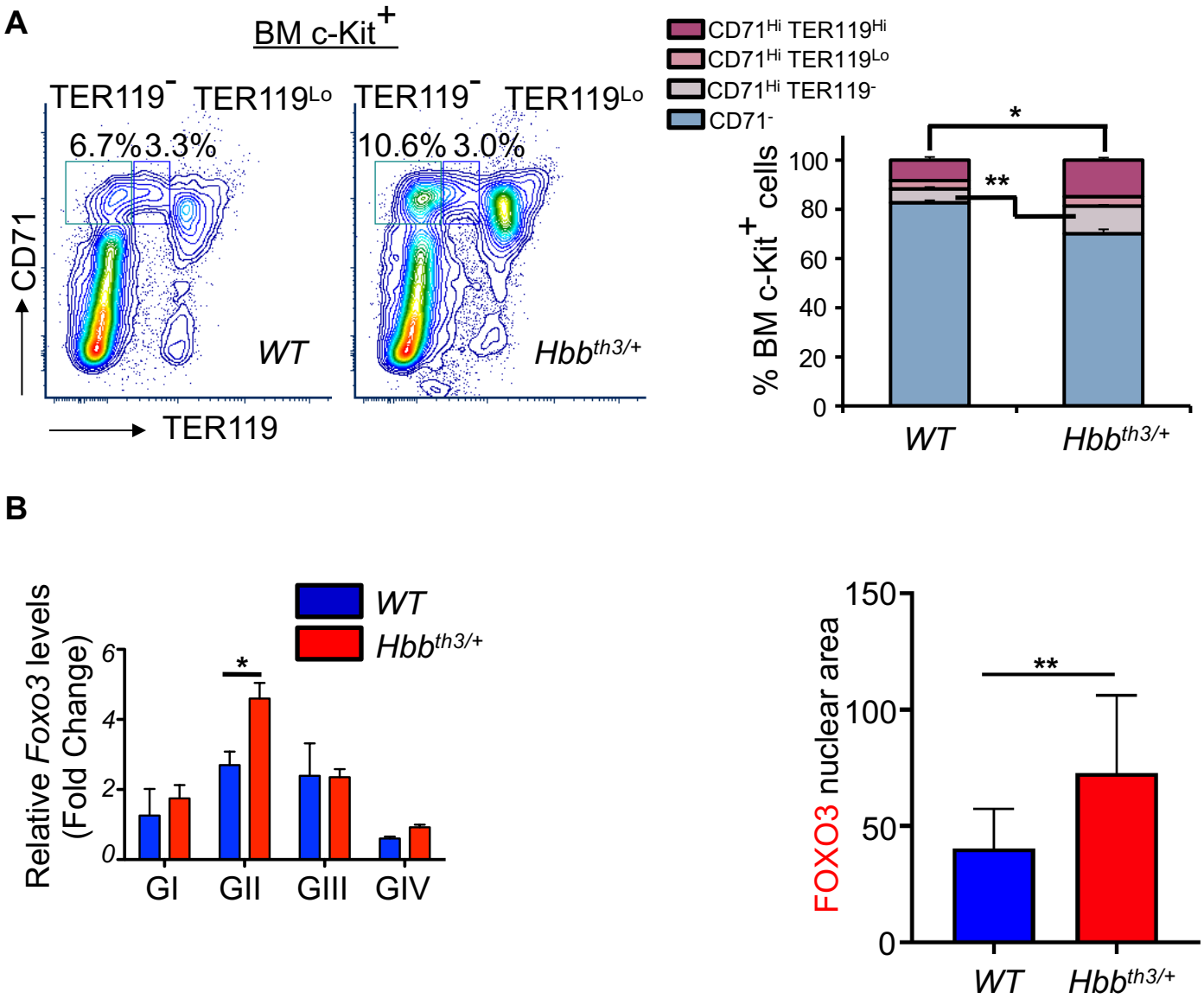
A
BM c-Kit+
TER119- TER119Lo
6.7% 3.3%
TER119- TER119Lo
10.6% 3.0%
CD71
TER119
WT
Hbbth3/+
CD71Hi TER119Hi
CD71Hi TER119Lo
CD71Hi TER119-
CD71-
% BM c-Kit+ cells
*
**
WT
Hbbth3/+
B
Relative Foxo3 levels (Fold Change)
WT
Hbbth3/+
*
GI
GII
GIII
GIV
FOXO3 nuclear area
**
WT
Hbbth3/+
C
TER119- c-KIT+ CD71Hi
WT
Hbbth3/+
DAPI
FOXO3
Merge

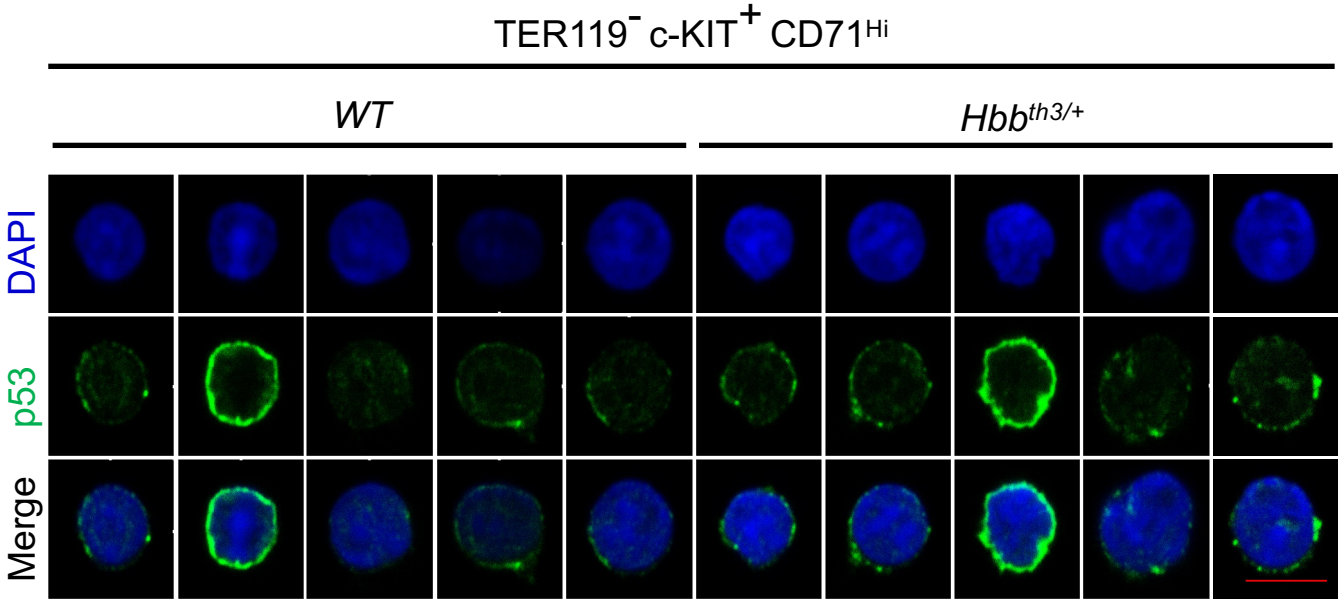
TER119- c-KIT+ CD71Hi
WT
Hbbth3/+
DAPI
p53
Merge

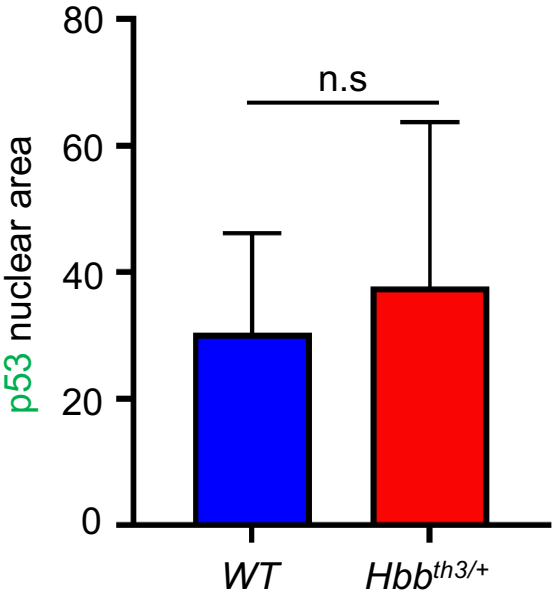
p53 nuclear area
80
60
40
20
0
n.s
WT
Hbbth3/+

A

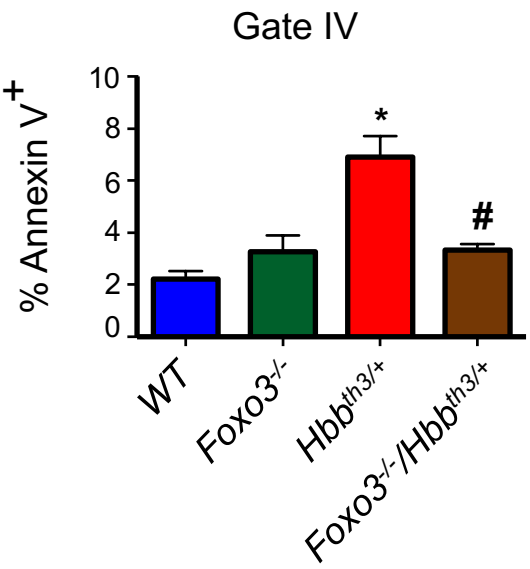
Gate IV
% Annexin V+
10
8
6
4
2
0
*
#
WT
Foxo3-/-
Hbbth3/+
Foxo3-/-/Hbbth3/+

B

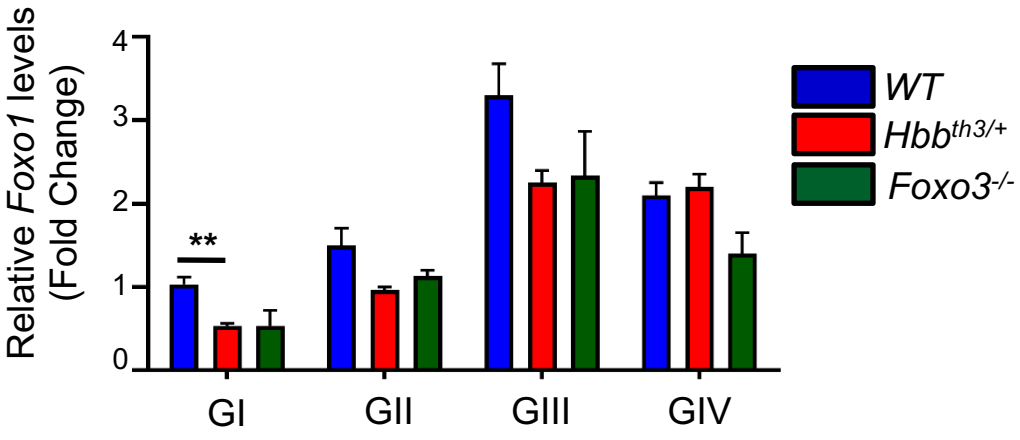
Relative Foxo1 levels
(Fold Change)
4
3
2
1
0
**
GI
GII
GIII
GIV
WT
Hbbth3/+
Foxo3-/-

A

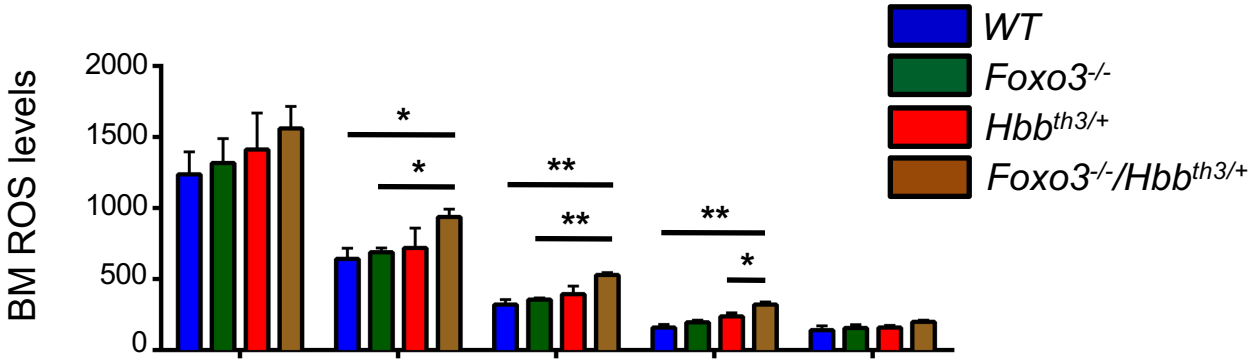
WT
Foxo3-/-
Hbbth3/+
Foxo3-/-/Hbbth3/+
BM ROS levels
2000
1500
1000
500
0
*
*
**
**
**
*

B

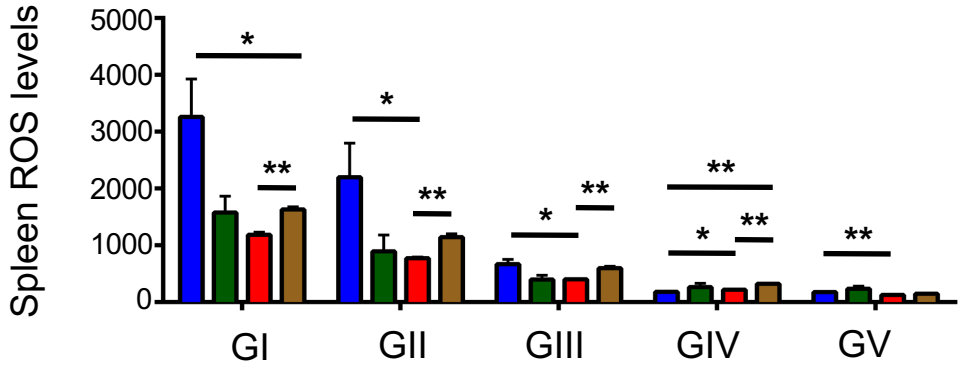
Spleen ROS levels
5000
4000
3000
2000
1000
0
*
**
*
**
*
**
*
**
*
**
GI
GII
GIII
GIV
GV

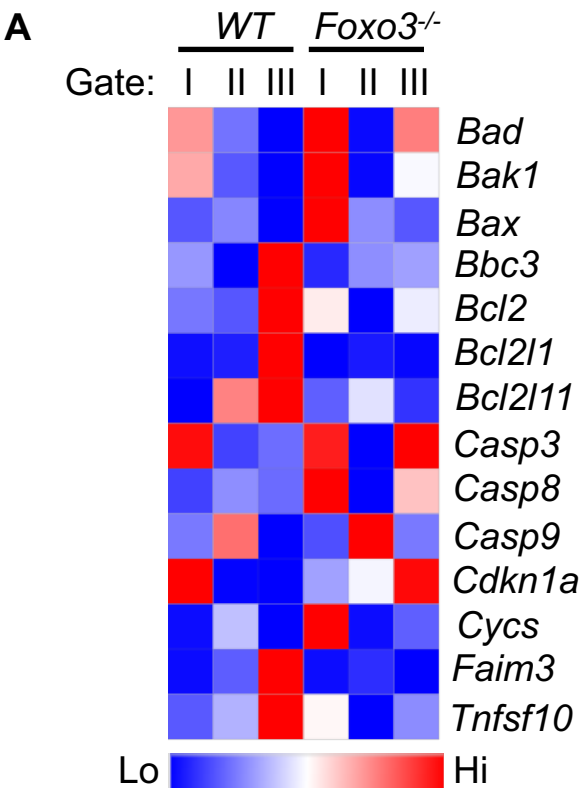
A
WT
Foxo3-/-
Gate: I II III I II III
Bad
Bak1
Bax
Bbc3
Bcl2
Bcl2l1
Bcl2l11
Casp3
Casp8
Casp9
Cdkn1a
Cycs
Faim3
Tnfsf10
Lo
Hi

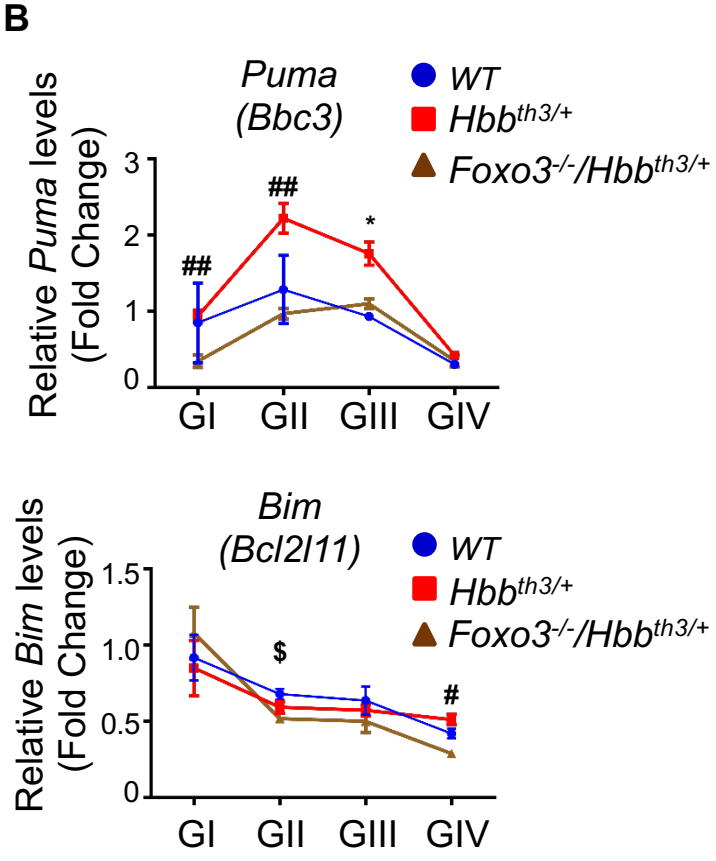
B
Puma (Bbc3)
WT
Hbbth3/+
Foxo3-/-/Hbbth3/+
Relative Puma levels (Fold Change)
GI GII GIII GIV
Bim (Bcl2l11)
Relative Bim levels (Fold Change)

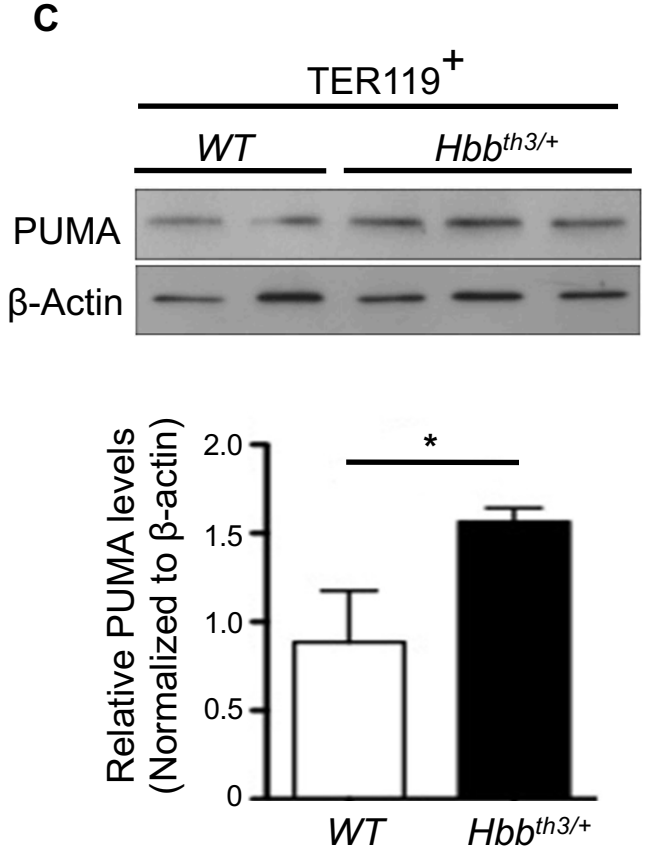
C
TER119+
WT
Hbbth3/+
PUMA
β-Actin
Relative PUMA levels (Normalized to β-actin)

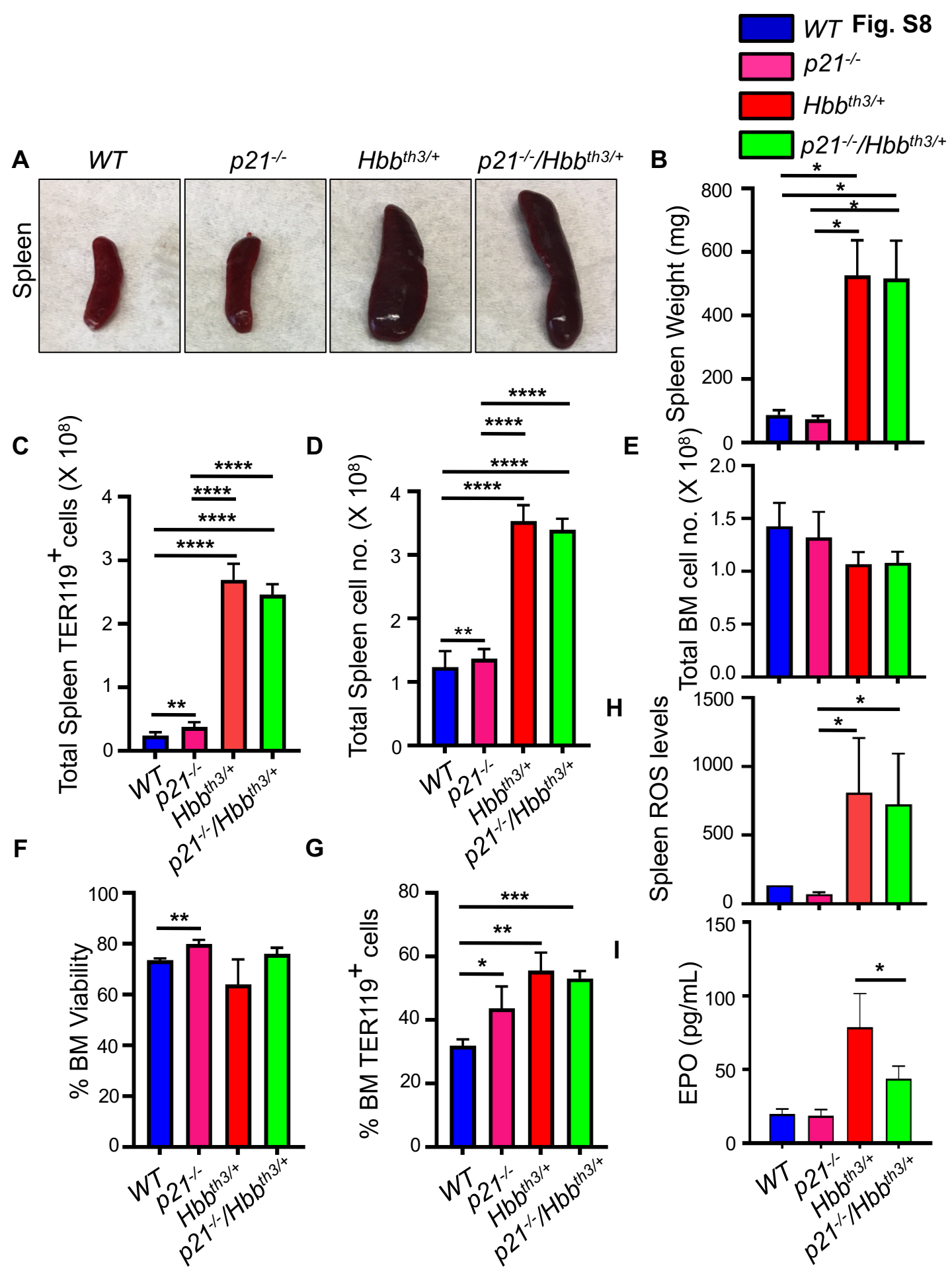
Fig. S8
WT
p21-/-
Hbbth3/+
p21-/-/Hbbth3/+
A
Spleen
B
Spleen Weight (mg)
C
Total Spleen TER119+ cells (X 10^8)
D
Total Spleen cell no. (X 10^8)
E
Total BM cell no. (X 10^8)
F
% BM Viability
G
% BM TER119+ cells
H
Spleen ROS levels
I
EPO (pg/mL)

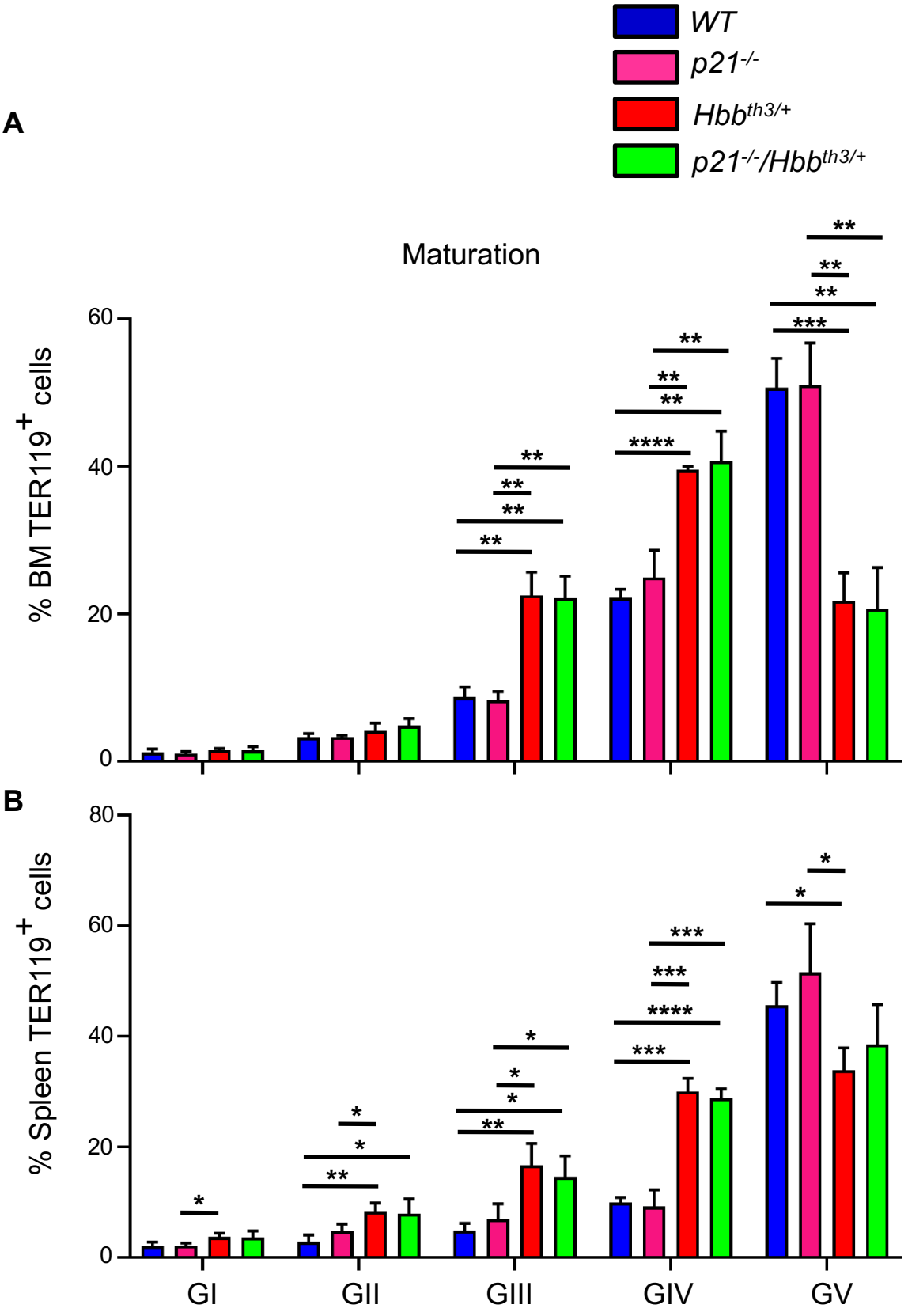
WT
p21-/-
Hbbth3/+
p21-/-/Hbbth3/+
A
Maturation
% BM TER119+ cells
60
40
20
0
B
% Spleen TER119+ cells
80
60
40
20
0
GI
GII
GIII
GIV
GV